

Electrospun nanofiber scaffolds: engineering soft tissues

This article has been downloaded from IOPscience. Please scroll down to see the full text article.

2008 Biomed. Mater. 3 034002

(<http://iopscience.iop.org/1748-605X/3/3/034002>)

[The Table of Contents](#) and [more related content](#) is available

Download details:

IP Address: 155.37.237.235

The article was downloaded on 12/04/2010 at 15:09

Please note that [terms and conditions apply](#).

Electrospun nanofiber scaffolds: engineering soft tissues

S G Kumbar¹, R James², S P Nukavarapu¹ and C T Laurencin^{1,2,3}

¹ Department of Orthopaedic Surgery, University of Virginia, VA 22908, USA

² Department of Biomedical Engineering, University of Virginia, VA 22908, USA

³ Department of Chemical Engineering, University of Virginia, VA 22904, USA

E-mail: laurencin@virginia.edu

Received 2 August 2007

Accepted for publication 1 October 2007

Published 8 August 2008

Online at stacks.iop.org/BMM/3/034002

Abstract

Electrospinning has emerged to be a simple, elegant and scalable technique to fabricate polymeric nanofibers. Pure polymers as well as blends and composites of both natural and synthetics have been successfully electrospun into nanofiber matrices. Physiochemical properties of nanofiber matrices can be controlled by manipulating electrospinning parameters to meet the requirements of a specific application. Such efforts include the fabrication of fiber matrices containing nanofibers, microfibers, combination of nano–microfibers and also different fiber orientation/alignments. Polymeric nanofiber matrices have been extensively investigated for diversified uses such as filtration, barrier fabrics, wipes, personal care, biomedical and pharmaceutical applications. Recently electrospun nanofiber matrices have gained a lot of attention, and are being explored as scaffolds in tissue engineering due to their properties that can modulate cellular behavior. Electrospun nanofiber matrices show morphological similarities to the natural extra-cellular matrix (ECM), characterized by ultrafine continuous fibers, high surface-to-volume ratio, high porosity and variable pore-size distribution. Efforts have been made to modify nanofiber surfaces with several bioactive molecules to provide cells with the necessary chemical cues and a more *in vivo* like environment. The current paper provides an overlook on such efforts in designing nanofiber matrices as scaffolds in the regeneration of various soft tissues including skin, blood vessel, tendon/ligament, cardiac patch, nerve and skeletal muscle.

(Some figures in this article are in colour only in the electronic version)

1. Introduction

Nanotechnology is a new technological endeavor that combines the study, control, manipulation and assembly of multifarious nanoscale components into materials, systems and devices to serve human interest and needs (Berne 2004). This emerging field has potential applications in many sectors of the global economy including consumer products, health care, transportation, energy and agriculture. Nanotechnology has revolutionized many branches of science such as surface microscopy, silicon fabrication, biochemistry, molecular biology, physical chemistry and computational engineering. Nanotechnology deals with natural and artificial structures on the nanometer scale, i.e., in the range from

1 μm down to 1 nm. Nanodimensions impart unusual properties as compared to conventional macro sized and bulk materials. Some of these unusual properties exhibited by nano structures include an extraordinarily high surface area to volume ratio, tunable optical emission and super paramagnetic behavior, which can be successfully exploited for a variety of health care applications ranging from drug delivery to biosensors. Several nano-sized materials or structures such as nanotubes, nanowires, nanocrystals, nanorods, nanocomposites, nanospheres and nanofibers received great deal of interest for various high technology applications (Fang *et al* 2005, Huang *et al* 2003, Kumbar *et al* 2008, Nalwa 2000, Nukavarapu *et al* 2008, Peppas *et al* 2007). Several nanoparticle-based products are available for biomedical and

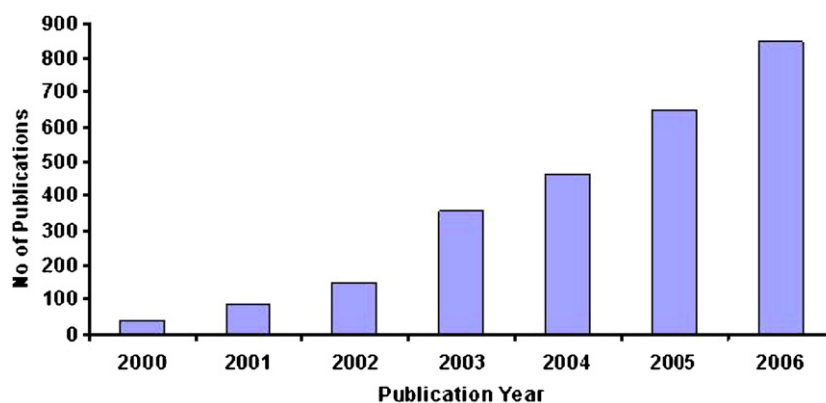


Figure 1. Graph showing research articles published in recent years using electrospun nanofibers. These numbers were based on the Sci-Finder Scholar search using the keywords electrostatic spinning, electrospinning and nanofibers. This graph clearly demonstrates the surging interest in nanofibers and related applications.

cosmetic applications including antimicrobials, bio-magnetic separations, bio-detection/labeling, drug/MRI contrast agents delivery, orthopaedics/implants, sunscreens and coatings (Fang *et al* 2005, Huang *et al* 2003, Kumbar *et al* 2008, Nalwa 2000, Nukavarapu *et al* 2008, Peppas *et al* 2007).

Nanofibers are being explored for a variety of applications and research in this area is rapidly expanding. A literature survey for nanofibers based on a Sci-Finder Scholar search in the past five years is presented in figure 1 and it clearly demonstrates the surging interest in nanofibers. Nanofibers have proven their potential applications in the field of filtration, sensors, military protective clothing, photovoltaic devices, liquid-crystal display (LCD), ultra-light weight space craft materials, super-efficient and functional catalysts and variety of biomedical and cosmetic applications (Burger *et al* 2006, Chew *et al* 2006, Chiu *et al* 2005, Huang *et al* 2003, Kumbar *et al* 2006, Laurencin and Nair 2004, Liao *et al* 2006). In biomedical applications, nanofibers have been used as carriers for drug/therapeutic agent delivery, wound dressing materials and as porous three dimensional scaffolds for engineering various tissues such as skin, blood vessels, nerve, tendon, bone and cartilage (Burger *et al* 2006, Chew *et al* 2006, Chiu *et al* 2005, Huang *et al* 2003, Kumbar *et al* 2006, Laurencin and Nair 2004, Liao *et al* 2006).

Generally fibers with diameters less than $1\ \mu\text{m}$ are termed as nanofibers. Nanofibers provide a connection between the nano and the macroscopic objects. Nanofibers due to their extremely high surface to mass ratio possess several novel properties such as low density, high pore volume, variable pore size and exceptional mechanical properties. These remarkable properties of nanofibers have led to the development of several non-woven applications. A current research emphasis is to develop nanofibers from a wide range of polymers and characterize them (Burger *et al* 2006, Chew *et al* 2006, Chiu *et al* 2005, Huang *et al* 2003, Kumbar *et al* 2006, Laurencin and Nair 2004, Liao *et al* 2006).

2. Electrospinning: fabrication of nanofiber matrices

Nanofibers are fabricated using a variety of fabrication techniques namely drawing (Nain *et al* 2006), template

synthesis (Tao and Desai 2007), temperature-induced phase separation (Liu *et al* 2005), molecular self-assembly (Paramonov *et al* 2006) and electrospinning (Hohman *et al* 2001a, 2001b, Reneker *et al* 2000, Yarin *et al* 2001a, 2001b). Among these, electrospinning appears to be a very reasonable technique to fabricate polymeric nanofibers from a variety of polymer solutions and melts (Ward 2001). ‘Electrospinning’ or ‘electrostatic spinning’ are two commonly used terminologies for this process, and in this paper, we use the more popular term electrospinning to maintain uniformity in the text. Electrospinning technique has several advantages over other nanofiber fabrication techniques listed in table 1. This process is simple, elegant, reproducible, continuous and scalable. It is possible to fabricate fibers in the diameter range of $\sim 3\ \text{nm}$ – $6\ \mu\text{m}$ and several meters in length using the same experimental set-up.

Electrospinning is aided by the application of high electric potentials of few kV magnitudes to a pendant droplet of polymer solution/melt from a syringe or capillary tube as presented in figure 2. In brief, a polymer jet is ejected from the surface of a charged polymer solution when the applied electric potential overcomes the surface tension. The ejected jet under the influence of applied electrical field travels rapidly to the collector and collects in the form of non-woven web as the jet dries. Before reaching the collector the jet undergoes a series of electrically driven bending instabilities (Hohman *et al* 2001a, 2001b, Reneker *et al* 2000, Yarin *et al* 2001a, 2001b) that results in a series of looping and spiraling motions. In an effort to minimize the instability due to the repulsive electrostatic forces, the jet elongates to undergo large amounts of plastic stretching that consequently leads to a significant reduction in its diameter and results in ultra-thin fibers. With low viscosity polymer solutions, the ejected jet may break down into droplets and result in electrospray (Kumbar *et al* 2007a). Therefore, a suitable polymer concentration is essential to fabricate nanofibers without any beads or beads-on-a string appearance. For instance, increase in viscosity or polymer concentration results in fiber diameter increase. By changing polymer concentration alone it is possible to fabricate the fiber diameters in the range of few nm to several micrometers while keeping other electrospinning parameters at a constant.

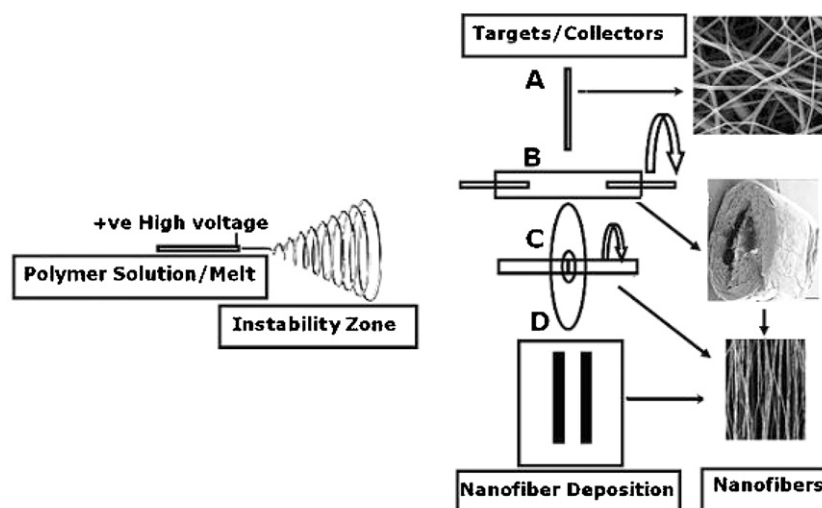


Figure 2. Schematics of electrospinning setup: a high electric potential of a few kV is applied to the pendent polymer droplet/melts and a polymer jet is ejected from the charged polymer solution. The polymer jet undergoes a series of bending and stretching instabilities that causes large amounts of plastic stretching, resulting in ultra-thin fibers. Based on the type of collector/target and its motion it is possible to align nanofibers. (A) Stationary collectors (grounded conductive substrate) result in random nanofibers. Rotating targets such as (B) a rotating drum and (C) wheel-like bobbin or metal frame result in fiber alignment and fabrication of tubular nanofiber scaffolds. (D) Example of a split electrode consists of two conductive substrates separated by a void gap that results in the deposition of aligned nanofibers across.

Table 1. Comparison of different nanofiber fabrication techniques: advantages and disadvantages.

Fabrication technique	Advantages	Disadvantages
Drawing	<ul style="list-style-type: none"> • Simple equipment 	<ul style="list-style-type: none"> • Discontinuous process • Not scalable • No control on fiber dimensions
Template synthesis	<ul style="list-style-type: none"> • Continuous process • Fiber dimensions can be varied using different templates. 	<ul style="list-style-type: none"> • Not scalable
Temperature-induced phase separation	<ul style="list-style-type: none"> • Simple equipment • Convenient to process • Mechanical properties of the fiber matrices can be varied by changing the polymer composition. 	<ul style="list-style-type: none"> • Limited to specific polymers • Not scalable • No control on fiber dimensions
Molecular self-assembly	<ul style="list-style-type: none"> • Only smaller nanofibers of few nm in diameter and few microns in length can be fabricated. 	<ul style="list-style-type: none"> • Complex process • Not scalable • No control on fiber dimensions
Electrospinning	<ul style="list-style-type: none"> • Simple instrument • Continuous process • Cost effective compared to other existing methods • Scalable • Ability to fabricate fiber diameters Few nm to several microns. 	<ul style="list-style-type: none"> • Jet instability • Toxic solvents • Packaging, shipping, handling

Various parameters that potentially affect electrospinning include polymer molecular weight, polymer solution properties, applied electrical potential, polymer solution flow rate, distance between spinneret and collector (working distance), motion of the grounded target and ambient parameters (temperature, humidity and air velocity). Nanofiber diameter, surface morphology, mechanical properties, porosity and pore-size distribution greatly depend on these parameters selected for electrospinning. Various polymers of both synthetic and natural origin have been successfully electrospun into nanofiber matrices (Burger *et al*

2006, Chew *et al* 2006, Chiu *et al* 2005, Huang *et al* 2003, Kumbar *et al* 2006, Laurencin and Nair 2004, Liao *et al* 2006). Most of the nanofiber fabrication techniques systematically varied polymer viscosity, applied voltage, working distance or flow rate one at a time while keeping the other parameters constant in an effort to optimize electrospun nanofibers with desired physiochemical properties (Burger *et al* 2006, Chew *et al* 2006, Chiu *et al* 2005, Huang *et al* 2003, Kumbar *et al* 2006, Laurencin and Nair 2004, Liao *et al* 2006). Among these parameters, polymer solution concentration/viscosity, conductivity, applied electrical potential and the effect

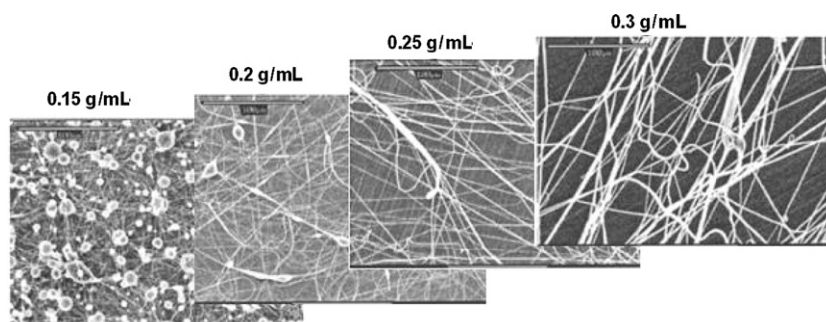


Figure 3. SEM micrographs of PLAGA fiber matrices electrospun at various polymer solution concentrations while using constant spinning parameters at an applied voltage of 20 kV cm^{-1} , a flow rate of 2 mL h^{-1} and ambient parameters. Increasing polymer concentration ($0.15\text{--}0.3 \text{ g mL}^{-1}$) implies an increase in polymer viscosity, resulted in decrease of bead density and concentration 0.25 g mL^{-1} resulted in bead-free nanofibers and fiber diameter increased beyond that concentration. Reprinted with permission from © 2004 Wiley Periodicals, Inc. (Katti *et al* 2004).

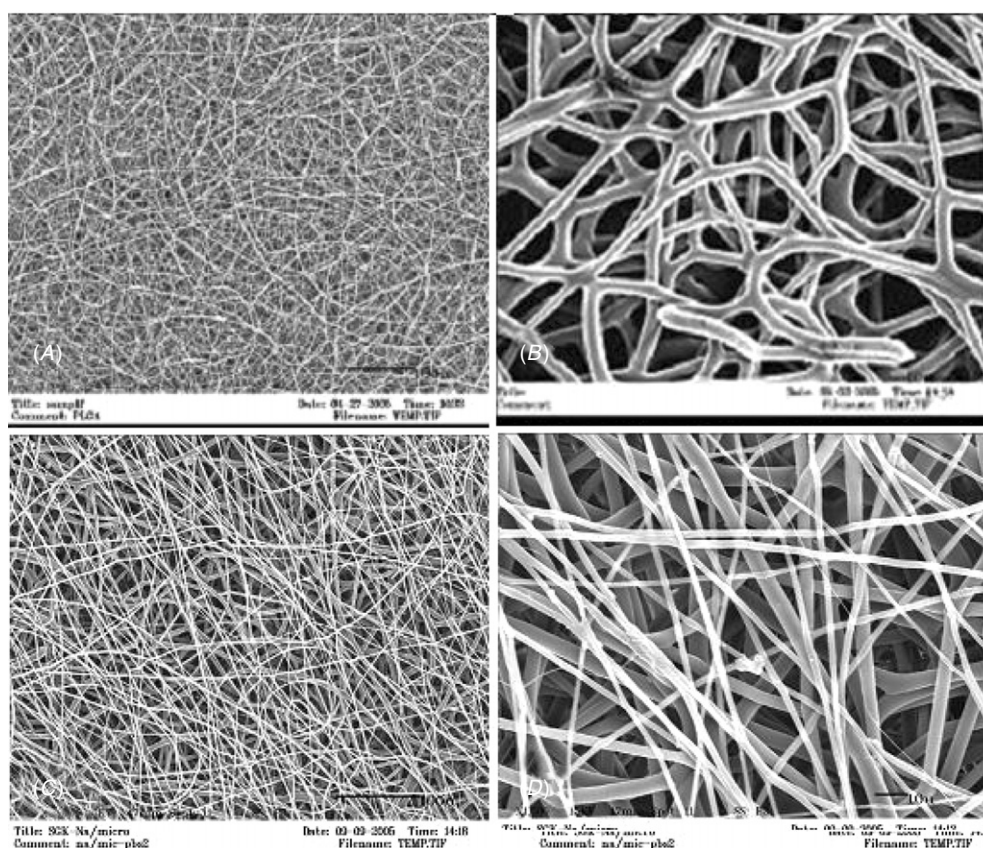


Figure 4. SEM micrographs of PLAGA fiber matrices electrospun at various polymer solution concentrations while using constant spinning parameters at an applied voltage of 20 kV cm^{-1} , a flow rate of 2 mL h^{-1} and ambient parameters. Where (A) nanofibers (0.22 g mL^{-1}), (B) microfibers (0.42 g mL^{-1}), (C) and (D) were produced by co-spinning of two different concentrations: (C) nanofibers (0.22 g mL^{-1})–microfibers (0.32 g mL^{-1}) and (D) nanofibers (0.22 g mL^{-1})–microfibers (0.42 g mL^{-1}).

of target geometry/motion that essentially determines the nanofiber morphology and physical properties will be discussed.

Electrospinning system parameters namely polymer and polymer solution properties play a significant role in controlling the fiber diameter and structural morphology. For instance, Laurencin and coworkers dissolved poly(lactide-*co*-glycolide) (PLAGA, $M_w = 56\,000$) in a solvent mixture of tetrahydrofuran (THF): dimethylformamide (DMF) (3:1) to obtain concentration ranges $0.1\text{--}0.3 \text{ g mL}^{-1}$ and were

electrospun while keeping the electrical potential constant at 1 kV cm^{-1} (Katti *et al* 2004). Polymer concentration of 0.1 , 0.15 and 2 g mL^{-1} resulted in bead-fiber structures; however bead density decreased with increasing polymer concentration (viscosity). Polymer concentrations beyond 0.25 g mL^{-1} resulted in bead-free nanofibers as shown in figure 3.

Ongoing studies in the Laurencin laboratories have successfully demonstrated the feasibility of developing nano, micro and, nano–microfibers simply by varying the polymer concentration/viscosity while keeping other

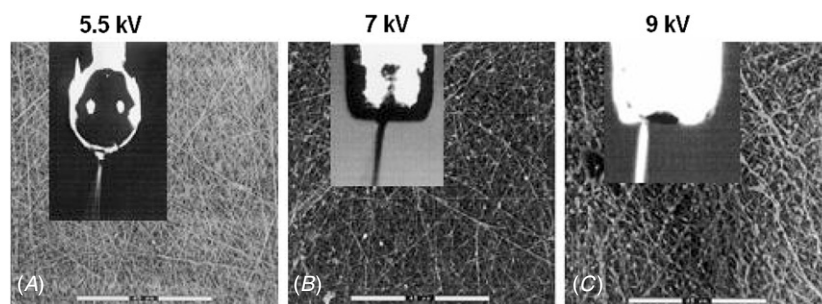


Figure 5. SEM micrographs of PEO nanofibers electrospun at a polymer concentration of 7 wt% while varying the electrospinning voltages from 5.5 to 9 kV. Where (A) an applied voltage of 5.5 kV, a droplet of solution, remains suspended at the end of the syringe needle, and the fiber jet originates from a cone at the bottom of the droplet results in bead-free nanofibers. (B) At 7 kV the jet originates from the liquid surface within the syringe tip and results in beaded nanofibers. (C) At 9 kV, the jet appears to be initiating directly from the tip with no externally visible droplet or cone and results in the formation of greater number of beads. Reprinted with permission from Copyright © 2001 Elsevier Ltd. (Deitzel *et al* 2001).

parameters constant as shown in figure 4. Authors have also demonstrated electrospinning using less viscous PLAGA solutions to coat various biomedical implants (Kumbar *et al* 2007a). Similar observations were made for many other polymer systems and these studies indicate the existence of optimal polymer concentration (viscosity) for electrospinning (Burger *et al* 2006, Chew *et al* 2006, Chiu *et al* 2005, Huang *et al* 2003, Kumbar *et al* 2006, Laurencin and Nair 2004, Liao *et al* 2006).

Polymer solution conductivity also plays an important role in electrospinning and determines nanofiber morphology and fiber diameter. Functional groups on polymer backbone, solvents used and presence of ionic species in the solution system determine the conductivity of polymer solution. Conducting polymer solutions carries more electrical charge and generates stronger repulsive forces on the polymer jet, and thus polymer solutions with ionic salts resulted in bead-free uniform fibers while a pure polymer—solvent systems—had many beads with fibers (Kim *et al* 2005).

Process parameters such as electrical potential, flow rate, working distance ambient parameters and motion of the target also play a vital role in dictating the fiber diameter, structure morphology and fiber alignment. Polymer properties and applied electrical potentials have pronounced an effect on polymer jet initiation and mode of jet instability, which effectively produces changes in the fiber morphology. Applied electrical potential during electrospinning directly translates into electrospinning current and results in different modes of jet initiation and instabilities (Shin *et al* 2001). An increase in applied electrical potential causes an increase in spinning current, and hence a corresponding increase in the mass flow rate from the capillary tip to the grounded collector when all other variables (polymer solution conductivity and flow rate) are held constant (Deitzel *et al* 2001). For instance, in a polyethylene oxide/water system where the applied electrical potential was increased from 5.5 kV to 9 kV, an increase in spinning current was observed, and the fiber morphology changed from defect-free fibers to a highly beaded structure (Deitzel *et al* 2001). Figure 5 presents the various modes of jet initiation and morphology of the nanofibers at various applied electrical potentials (Deitzel *et al* 2001). For different polymer

systems these process parameters need to be considered to obtain defect-free uniform nanofibers and several studies have been reported that indicate the importance of these parameters (Burger *et al* 2006, Chew *et al* 2006, Chiu *et al* 2005, Huang *et al* 2003, Kumbar *et al* 2006, Laurencin and Nair 2004, Liao *et al* 2006).

During electrospinning electrostatic forces such as strong external field, the collector type and charges exerted by adjacent fibers mainly control the motion of fibers ejected from the polymer jet. Nanofiber deposition can be done on a stationary (a piece of grounded conductive substrate) target or a rotating target such as a rotating drum, wheel-like bobbin or metal frame (Theron *et al* 2001, Bhattacharyya *et al* 2006, Katti *et al* 2004, Zhang *et al* 2007). Often randomly oriented nanofiber deposition was possible with stationary target due to the non-preferential direction for electrostatic forces (Hohman *et al* 2001a, 2001b, Reneker *et al* 2000, Yarin *et al* 2001a, 2001b). When a rotating target replaced a stationary target, it was possible to align nanofibers more or less parallel to each other (Theron *et al* 2001, Bhattacharyya *et al* 2006, Zhang *et al* 2007). With a rotating drum collector the linear rotating speed serves as a fiber take-up device, and when the rotational speed matches the evaporated jet depositions, the fibers are taken up on the cylindrical surface in a circumferential manner resulting in a fair alignment (Theron *et al* 2001, Bhattacharyya *et al* 2006, Zhang *et al* 2007). In the case of the wheel-like bobbin collector, charge accumulation on the tip-like edges attracts fibers continuously, which winds up on the bobbin edge of the rotating wheel (Theron *et al* 2001). Several other attempts to align nanofibers made use of frame collectors (Dalton *et al* 2005, Fridrikh *et al* 2003, Li *et al* 2004), and patterned electrodes (Li *et al* 2005) that essentially provide preferential direction for electrostatic forces controlling the motion of the fibers.

3. Mechanical properties of electrospun nanofiber matrices

Nanofiber matrices need to possess adequate mechanical properties to be effective in any application. A wide range of polymers of both natural and synthetic origin,

alone or in combination has been successfully electrospun into nanofiber matrices using different fabrication conditions and parameters. Nanofiber alignments, fabrication of core-shell nanofibers, hollow nanofibers and combinations of nanofibers of different polymers (co-spinning) have also been fabricated by altering the electrospinning equipment. Electrospun nanofiber matrices due to their high surface area and tiny pores possess a wide range of mechanical properties which is entirely different from original bulk materials. Mechanical properties of fiber matrices depend on the chemical composition, fabrication procedure, fiber diameter and their alignment. Knowledge of strain–stress behavior of nanofiber matrices gives an understanding about their performance in the desired application under dynamic stress. For instance, poly(3-hydroxybutyrate-co-3-hydroxyvalerate) (PHBV) nanofiber matrices with a specific surface area $140 \text{ m}^2 \text{ g}^{-1}$ and 70% porosity showed Young's modulus $350 \pm 30 \text{ MPa}$, tensile strength $8.6 \pm 0.8 \text{ MPa}$ and elongation at break 19.5 ± 1.5 . While PHBV cast films showed Young's modulus $3190 \pm 300 \text{ MPa}$, tensile strength 31 ± 3 and elongation at break 3.2 ± 0.5 (Kwon *et al* 2007). Fiber alignment in nanofiber matrices significantly improves the mechanical properties. For instance, poly(ϵ -caprolactone) non-aligned nanofiber matrices had a tensile modulus of $2.1 \pm 0.4 \text{ MPa}$. Fiber alignment was more pronounced when the mandrel speed was increased from 4.0 to 8.0 m s^{-1} and the resulting nanofibers showed tensile moduli 7.2 ± 0.6 and 11.6 ± 3.1 , respectively (Li *et al* 2007). Co-spinning of PLAGA and chitosan was achieved using dual power sources and nanofiber matrices with chitosan were cross linked with glutaraldehyde vapors (Duan *et al* 2007). PLAGA-chitosan nanofiber matrices showed improved mechanical properties than their parent polymers alone. PLAGA and chitosan nanofiber matrices showed a tensile strength of 2.5 MPa and 1.25 MPa , Young's modulus of 2.5 MPa and 40 MPa , and the percentage elongation of 42% and 3%, respectively. While co-spun PLAGA-chitosan nanofiber matrices showed a tensile strength of 1.3 MPa , Young's modulus of 110 MPa and the percentage elongation of 50% that are intermediate to the parent polymer nanofiber matrices (Duan *et al* 2007). Appropriate choice of polymer, suitable fabrication approach, varying fiber diameter composition, aligning fibers and nanofiber cross-linking are some of the currently used strategies to alter the mechanical properties of the nanofiber meshes. Such efforts can produce mechanical properties to meet the requirements of the tissue that they seek to regenerate.

4. Electrospun nanofiber matrices as tissue engineering scaffolds

It is clear from the literature that nanotopographical features significantly alter cell behavior. Nanotopographical features namely pores, ridges, groves, fibers, nodes and combinations of these features influenced cellular adhesion (Glass-Brudzinski *et al* 2002), morphology (Karuri *et al* 2004, Vitte *et al* 2004), proliferation (Dalby *et al* 2002), endocytotic activity (Dalby *et al* 2002), motility (Chen *et al* 1997) and gene expression (Chou *et al* 1998, Glass-Brudzinski *et al* 2002) of

various cell types. Various nanotopographical features have been created and used as new generation tissue engineering scaffolds and biomedical implant surfaces (Kumbar *et al* 2008). Basement membranes are unique extra-cellular matrices that support cell adhesion and provide an environment for the cells to interact with the surroundings. The ECM is composed of specific proteins, several functional groups, and growth factor reservoirs along with many tropic agents that are responsible for cellular function. Several cellular activities such as adhesion, proliferation, migration, differentiation and cell shape are influenced by the ECM in which the cells reside (Adams 2001, Chiquet 1999, Streuli 1999, Watt 1986). The ECM is principally composed of hierarchically arranged collagen, laminin, other fibrils and proteoglycans in a complex topography in the nanometer range. The basement urothelium membranes of rhesus macaque have topographical features in nanodimensions characterized by a height of $178 \pm 57 \text{ nm}$, interpore distance of $127 \pm 54 \text{ nm}$, fiber diameters of $52 \pm 28 \text{ nm}$ and pore diameters of $82 \pm 49 \text{ nm}$ (Abrams *et al* 2000, 2003). Electrospun nanofiber matrices show morphological similarities to the natural ECM, characterized by ultrafine continuous fibers, high surface-to-volume ratio, high porosity and variable pore-size distribution similar to the dimensions of basement membranes. Nanofiber matrices as tissue engineering scaffolds need to have interconnected highly porous structures to facilitate cellular migration and transport of nutrients, and metabolic wastes to allow the formation of new tissue. Electrospun nanofiber matrices present a dynamic system in which the pore size and shape can change when compared to other rigid porous structures. Laurencin and coworkers using mercury porosimetry determined PLAGA nanofibers to have a 91.63% porosity, a total pore volume of 9.69 mL g^{-1} , total pore area of $23.54 \text{ m}^2 \text{ g}^{-1}$ and a pore diameter ranging from 2 to $465 \mu\text{m}$ (Li *et al* 2002). The remarkable nanotopographic features of the nanofiber matrices provide cells the necessary physical cues similar to the nanotopographical features of a natural basement membrane. Polymeric nanofiber matrices can also act as carriers for a variety of bioactive agents including antibiotics, antifungal, antimicrobial, proteins (enzymes, DNA, etc), anticancer and other valued drugs (Kumbar *et al* 2006). Core-shell nanofibers have been successfully designed to release the desired bioactive agents at therapeutic concentrations in both a spatial and temporal pattern (Jiang *et al* 2005). Recently Jayasinghe *et al* have successfully demonstrated the feasibility of encapsulating living cells within core-shell microfiber matrices (Jayasinghe *et al* 2006, 2007) These microfiber matrices obtained via cell electrospinning showed significant numbers of viable cells over long periods of time. Thus, nanofiber matrices encapsulated with suitable growth factors, cells or bioactive agents have a great potential for use in tissue regeneration by providing cells with necessary physical and chemical cues. In this paper we will make an effort to summarize the efforts made by several researchers to regenerate various soft tissues such as skin, blood vessel, tendon/ligament and nerve using electrospun nanofibers.

4.1. Electrospun nanofiber skin grafts

Tissue engineering has emerged as an alternative treatment to traditional autografts and allografts for excessive skin loss. Such an approach involves scaffolds, cells and biological factors alone or in combination (MacNeil 2007). Electrospun nanofiber scaffolds due to their high surface area-to-volume ratio provide more surface for cell attachment compared to other structures from the same material. In addition, nanofiber scaffolds are extensively used as wound dressings since they protect the wound area from the loss of fluid and proteins, aid in removal of exudates, inhibit exogenous microorganism invasion, improve appearance and have excellent anti-adhesion properties (Khil *et al* 2003, Zhang *et al* 2005a, Zong *et al* 2004). Polyurethane nanofiber matrices used as wound dressing materials in a rat skin defect model showed increased rate of epithelialization with well-organized dermis which provided good support for wound healing (Khil *et al* 2003). PLAGA nanofiber matrices in a rat model showed an excellent anti-adhesion effect and prevented complete cecal adhesions (Zong *et al* 2004). Several polymers of both natural and synthetic origins, alone or in combination, were successfully electrospun into nanofiber scaffolds, and evaluated as dermal substitutes with cells.

Collagen nanofibers play a dominant role in maintaining the biological and structural integrity of various tissues and organs, including bone, skin, tendon, blood vessels and cartilage. Glutaraldehyde cross-linked collagen type I nanofibers in the diameter range of 100–1200 nm showed tensile strengths of 11.44 ± 1.20 MPa close to several commercially available wound care products such as Beschitin[®] (15.89 ± 0.63 MPa) and Resolut[®] LT (11.72 MPa) (Rho *et al* 2006). Cross linking collagen nanofibers resulted in decrease of porosity from 89% to 71%. Relatively, less human keratinocytes and fibroblasts adhesion was observed on these cross-linked collagen nanofibers than the nanofiber matrices treated with type I collagen or laminin. Such an effect might be due to electrospinning collagen with a fluorinated solvent, and glutaraldehyde cross linking resulting in structural changes. However, coating these nanofiber matrices with ECM proteins, primarily collagen type I provided bioactivity and resulted in best *in vitro* performance. Collagen coated nanofiber matrices showed faster early-stage healing compared to the control group (cotton gauze) in full thickness wounds in a rat model. Blended nanofibers of collagen and polycaprolactone (PCL) supported growth, proliferation and migration of fibroblasts inside the matrices (Venugopal and Ramakrishna 2005). Surface modification of PCL nanofiber matrices with collagen was achieved using a dip coating method and by a core-shell nanofiber fabrication technique. Core-shell nanofibers had a collagen shell and PCL as the wrapped core. Collagen coating showed linearly increasing fibroblast density with time as compared to PCL nanofibers (Zhang *et al* 2005b). Collagen-PCL core-shell nanofibers had comparatively higher cell density than the nanofibers coated by dip coating, presumably due to the uniform collagen coating on the core-shell structures. Fibroblast adhesion was lower on aligned collagen nanofibers but showed higher proliferation when

compared with the random collagen nanofibers (Zhong *et al* 2006).

Electrospun silk fibroin (SF) nanofibers with diameters in the range of 30–120 nm showed 76.1% porosity (Kim *et al* 2003, Min *et al* 2004, 2006). These SF nanofiber matrices were treated with water vapor and methanol to provide structural stability and improve their mechanical properties. For instance, mechanical properties of SF untreated nanofibers showed a tensile modulus of 17.7 ± 6.8 MPa, while treatment with water vapor and methanol showed a tensile modulus of 30.4 ± 4.4 and 104.3 ± 13.7 MPa, respectively (Min *et al* 2006). Water vapor treatment provided a way to control conformational changes of SF nanofiber and these matrices supported the adhesion and spreading of normal human keratinocytes and fibroblasts (Min *et al* 2004, 2006). The highly porous chemically treated SF nanofiber matrices with high surface area, wide range of pore size distribution and improved mechanical properties are highly attractive as wound dressing materials and for skin regeneration applications (Kim *et al* 2003, Min *et al* 2004, 2006). Chitin/SF blend nanofibers at a blend composition of 75% chitin and 25% SF showed highest attachment and spreading for human keratinocytes and fibroblasts (Park *et al* 2006).

Electrospun chitin nanofibers and commercially available chitin microfibrils having fiber diameters of 163 nm and $8.77 \mu\text{m}$, showed fiber-size-dependent cell behavior. Chitin nanofibers showed a relatively higher attachment and spreading behavior of normal human keratinocytes and fibroblasts. Collagen type I coating further improved the efficacy of the nanofiber mats to promote cell attachment and proliferation. Chitin nanofibers completely degraded within 28 days into rat subcutaneous implantation without any inflammatory response (Noh *et al* 2006). Such an observed phenomenon may be due to the high surface area of nanofibers compared to microfibrils (Noh *et al* 2006).

PLAGA-dextran electrospun nanofibers supported fibroblast attachment, proliferation, migration and extracellular matrix deposition within the nanostructures as presented in figure 6. Fibroblasts migrated into these three-dimensional structures and organized into dense multi-layered structures resembled dermal architecture (Pan *et al* 2006).

Nanofibers of poly(p-dioxanone-co-L-lactide)-block-poly(ethylene glycol) with average diameters of 380 nm, median pore size $8 \mu\text{m}$, porosity >80% and mechanical strength 1.4 MPa supported fibroblast adhesion, proliferation and maintained phenotypic shape and guided growth along the nanofiber orientation (Bhattarai *et al* 2004). In an effort to develop a fibroblast-populated three-dimensional dermal analogue; blends of PCL/gelatin were electrospun onto a polyurethane dressing (Tegaderm, 3M Medical) (Chong *et al* 2007). The significant number of fibroblasts adhered and proliferated on both the sides of the construct and shows great potential in the treatment of dermal wounds through layered application. The surface-modified polyamide nanofibers coated with ECM proteins namely fibronectin, collagen I and laminin-1 supported primary mouse embryonic fibroblasts adhesion and proliferation better than tissue culture polystyrene (TCPS) protein-coated surfaces (Ahmed *et al*

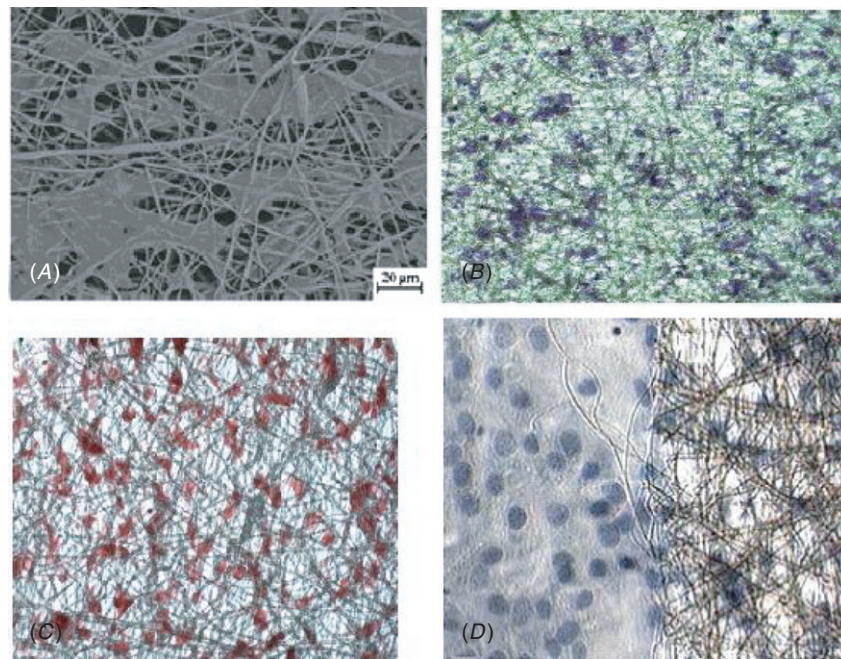


Figure 6. (A) SEM micrograph where fibroblasts present a well-spread morphology after three days of culture. (B) Optical micrograph showing fibroblasts distribution throughout the nanofiber scaffolds after one day culture where samples were stained with crystal violet. (C) and (D) optical micrographs showing deposition of collagen (Sirius Red staining) and elastin (Verhoeff's solution) staining. Reprinted with permission from Copyright © 2006 Elsevier Ltd. (Pan *et al* 2006).

2007). Co-culture of keratinocytes, fibroblasts and endothelial cells on polystyrene nanofiber scaffolds resulted in scaffolds populated with viable cells, even under serum-free conditions (Ahmed *et al* 2007). Fibroblasts may provide supportive environment for keratinocyte and endothelial cell viability under serum-free conditions. Cells presented native spatial three-dimensional organization where keratinocytes formed a continuous 'epidermal' layer at the upper air-facing surface, while fibroblasts and endothelial cells occupied the central and lower regions (Ahmed *et al* 2007). Electrospun polyamide nanofibers were surface modified by coating with ECM proteins namely fibronectin, collagen I and laminin-1, and they supported primary mouse embryonic fibroblasts adhesion and proliferation better than the TCPS-protein-coated surfaces (Sun *et al* 2005). Nanofiber matrices provide a necessary 3D structure similar to natural ECM and result in better cell performance than 2D substrates. Laurencin and coworkers fabricated electrospun PLAGA fiber matrices in the diameter range of 150–225, 200–300, 250–467, 500–900, 600–1200, 2500–3000 and 3250–6000 nm and studied human skin fibroblast behavior in an effort to optimize the fiber diameter to produce skin grafts (Kumbar *et al* 2007). Fibroblasts showed fiber-size-dependent proliferation behavior and showed highest proliferation on scaffolds with a fiber diameter in the range of 600–1200 nm. These observations may be a combined effect of surface area, surface roughness, porosity and protein binding ability of the scaffolds. Collagen type III expression also showed fiber diameter dependence on its expression similar to the observed proliferation trend (Kumbar *et al* 2007c). Nanofiber matrices with suitable mechanical properties, degradation

profile, porosity, 3D architecture, necessary chemical cues and increased fibroblast and related cells response is required to produce skin substitutes.

4.2. Electrospun nanofiber blood vessel grafts

Following vascular injury, excessive extra-cellular matrix deposition leading to a pathological condition known as intimal hyperplasia may occur. When located in large diameter blood vessels, problems such as narrowing of the lumen and thus changes in blood flow are observed. However, very rarely does occlusion occur in large vessels. In smaller diameter vessels, this is a severe and often fatal condition as the vessels lack room for expansion during the remodeling phase. This pathological condition is best treated by bypass grafting procedures that use saphenous vein. Synthetic vascular grafts, such as polytetrafluoroethylene (PTFE) were investigated as small diameter blood vessel substitutes. These grafts have greatly reduced patency and thus high failure rates as they failed to mimic native graft functionality. Electrospinning techniques have shown potential to mass produce tubular scaffolds that would meet the functional requirements of native blood vessels. Blood vessels are tubular-shaped structures composed of oriented protein fibers and integrated cells, both smooth muscle (SMC) and endothelial cells (EC). Nanofiber-based engineered substitutes mimic the dimension scale and the spatial organization of the 3D ECM features of native tissue, and may be made suitable for interaction with smooth muscle cells and endothelial cells (Kumbar *et al* 2007b). Blood vessels are composed of three distinct cellularized layers with abundant collagen and elastin. The circumferential orientation

of these ECM fibrils along with the aligned SMCs provides the necessary functional strength and compliance. Bio-mimicking engineered scaffolds may improve cellular integration, and in addition must satisfy the functional parameters under mechanically active conditions (Buttafoco *et al* 2006, Jeong *et al* 2007, Stitzel *et al* 2006, Venugopal *et al* 2005).

Aligned poly(L-lactid-co- ϵ -caprolactone), P(LLA-CL::75:25) nanofibrous scaffolds with an average fiber diameter of 500 nm modulate SMC's behavior to express contractile phenotype, spindle shape, orient and migrate along the aligned nanofibers (Xu *et al* 2004). Thick and thin α -actin and myosin filaments are positively stained within SMCs cultures on aligned nanofiber matrices as compared to the 2D cultures on the same scaffold material. These cytoskeleton proteins are visualized parallel to the nanofiber direction. These aligned scaffolds mimic the nanoscale features, and the oriented cell and fiber architecture found in native blood vessels. Gelatin grafting on polyethylene terephthalate (PET) non-woven nanofibrous meshes (200–600 nm average fiber diameter) increased the hydrophilicity of the scaffold which enabled endothelial cells to adopt a well-spread polygonal-shaped morphology (Ma *et al* 2005). Surface adhesion proteins characteristically expressed by ECs, e.g. PECAM, VCAM-1 and ICAM-1 were highly expressed on gelatin-grafted non-woven nanofiber PET matrices. Increased expression of PECAM is indicative of a greater degree of endothelization on this scaffold as compared to non-woven nanofiber PET matrices. PET has been extensively used as large diameter vascular prosthesis, but has not proven successful in replacing smaller diameter vessels. Gelatin grafting onto PET nanofiber surface holds great potential in developing successful substitutes for small diameter blood vessels (He *et al* 2005, 2006).

PLA/PCL bilayered tubular scaffolds with a PCL inner layer of randomly oriented microfibrils (1.5–6 μm) and a PLA outer layer composed of oriented fibers with diameters from 800 nm to 3 μm have been fabricated (Yarin *et al* 2001a). The outside is composed of concentric layers of circumferentially oriented PLA fibers analogous to the tunica media layer of blood vessels. The concentric inner layers of randomly oriented PCL fibers represent the elastic lamina and tunica intima layers of a blood vessel. The bilayered PLA/PCL scaffolds have a maximum stress of 4.3 MPa and an elastic deformation up to 10% strain, which is strong enough and may provide the compliance necessary for substitute blood vessels. Cellular attachment, spreading and proliferation are proven on this bi-layered scaffold using mouse fibroblasts and human venous myofibroblasts. The fibroblasts adhered and proliferated along the aligned fibrous network revealing high cellular densities on the outer layer as compared to the inner layer over 30 days of static culture.

Inferior vena cava of mongrel dogs were replaced with freeze-dried hybrid scaffolds composed of polyglycolic acid (PGA) non-woven tubular fabric and a copolymer gel of L-lactide and ϵ -caprolactone P(CL/LA::50/50) seeded with vascular myofibroblasts and smooth muscle cells harvested from the femoral veins of these dogs (Watanabe *et al*

2001). These tissue-engineered vascular autografts remained patent (no stenosis and occlusions) in the animals up to six months as investigated by angiographies. Histological examinations showed dense collagen fibers, organized elastic fibers and cellular components within the graft starting at three months post-implantation. Immunostaining revealed factor VIII positive staining at the luminal surface of the graft, which is indicative of an endothelial cell lining that promotes antithrombogenicity. Uneven distribution of anti-SMA and desmin beneath the endothelial lining is a positive indicator of smooth muscle cells within the graft.

SMCs (rat aorta) suspended in gelatin supplemented media were electrosprayed concurrently with poly(ester urethane) urea (PEUU) to microintegrate cells uniformly throughout the scaffold (100 μm thickness) (Stankus *et al* 2006). The integrated cells exhibited spread morphology and significantly higher cellular proliferation under static culture at one week timepoint as compared with TCPS. With thicker SMC integrated PEUU scaffolds (300–500 μm thickness), the scaffold interior was devoid of cells under static culture due to diffusional limitations of nutrients, waste and oxygen. In a perfusion bioreactor these thick scaffolds exhibited higher numbers of uniformly distributed cells throughout the scaffold. Under perfusion culture, the cells showed a well-spread morphology and more f-actin staining than static culture conditions.

PCL fiber meshes (10 μm thickness) of 250 nm average fiber diameter suspended on a wire ring supports attachment and contraction of neonatal rat cardiomyocytes *in vitro* (Shin *et al* 2004). On day 3, cardiomyocytes start to contract weakly and in an unsynchronized fashion. These contractions become stronger and synchronized as time progresses. Cardiomyocytes adhered and populated throughout the entire scaffold mesh, and stained positively for cardiomyocyte proteins, i.e., actin, tropomyosin and cardiac troponin-I (Ishii *et al* 2005). This highly porous non-woven PCL mesh functions as a temporary ECM that enabled the cells to adhere, spread and proliferate. In addition, this mesh did not restrict the contractile functions of the cardiomyocytes. The wire ring provides passive tension that supports maturation of the beating cardiomyocytes, and may improve handling of the construct. A functional myocardial patch with sufficient cardiac functions may be prepared by stacking a few layers of the construct that beat in a synchronized manner. PLAGA scaffolds of varying compositions (100 wt% PLLA, 75 wt% PLAGA (90:10) + 25 wt% PLLA, and 85 wt% PLAGA (75:25) + 15 wt% PEG-PLA) with an average fiber diameter of 1 μm were uniaxially stretched, and supported attachment of myocytes (Zong *et al* 2005). The most hydrophobic scaffold (PLLA) was found to be most suitable for myocyte attachment and development of the contractile machinery typical of well-connected cardiac tissues. Cells were visualized along the fiber direction with elongated nuclei surrounded my mature cytoskeleton (actin filaments). The chemical composition of the scaffolds regulated its surface properties and degradation rate, which regulated the cellular behavior both morphologically and functionally as determined by electrical activity. PLLA scaffolds have confirmed superior

performance as compared to PLAGA (90:10) + PLLA and PLAGA + PEG-PLA.

4.3. Electrospun nanofiber tendon grafts

Tendon injuries are the most common body trauma in the young and physically active population. Due to problems of incomplete healing and recurrent injury, significant disability and dysfunction can occur. Problems, such as limited availability of tendon autografts, inflammatory risks of allografts, failure of long-term tendon prosthesis and restricted reparative potential of injured tendons, leave replacement procedures of large defects unsatisfactory. The combination of tendon prosthesis with an autologous cell can generate a tendon tissue and thus may provide a better approach to the current tendon injury problems. Tendon prosthesis currently used (Dacron grafts, carbon fibers, Silastic sheets) does not meet the functional requirements of the regenerative tissue. Tissue engineering, using a biodegradable scaffold that will functionally support and provide stimuli to the regenerating tissue is a novel approach (Cao *et al* 2002, 2006, Ouyang *et al* 2002, 2003).

Hybrid nano–microfibrous scaffolds composed of knitted PLAGA (90/10) covered with randomly oriented electrospun PLAGA (65:35) modulate bone-marrow-derived stromal cells (BMSCs) to exhibit a higher expression of collagen-I, decorin and biglycan (Sahoo *et al* 2006). Stromal cells thus retain the potential to differentiate into tendon/ligament lineage on this novel nano–microfibrous scaffold. The nanofibers with diameters ranging from 300 to 900 nm covered the knitted scaffold made from 25 μm microfilaments. The hybrid scaffolds had an initial load to failure of 56.3 N which fell to 1.82 N by 14 days. BMSCs attached and proliferated well on the novel scaffold forming cellular aggregates that increased in size and fused with the adjacent ones.

Dry non-woven chitin fabric (10 mm \times 15 mm \times 4 mm) has an initial load to failure of 9.4 N, which is not significantly different from that under wet conditions in four weeks (Funakoshi *et al* 2006). However, the initial elongation under a load of 19.4% (dry conditions) is significantly lower than the 40.9% elongation measured at the end of four weeks of incubation in 10% FBS supplemented DMEM. The fabric used as a rotator cuff replacement in rabbits showed dense regenerative tissue and collagen bundles along the direction of force in four weeks. In 8–12 weeks, the chitin was absorbed and the characteristic crimp pattern of oriented collagen fibrils was evident. At all time points there was minimal evidence of an inflammatory response to the chitin fabric. Chitin implants promote aggressive tissue ingrowth whereas the polylactic acid implants have poor tissue ingrowth in a rabbit Achilles tendon defect model (Sato *et al* 2000). Load to the failure of the grafted shoulder was 135.4 N which is significantly higher than the 12.9 N measured at the control shoulder.

4.4. Electrospun nanofiber nerve grafts

Peripheral nerve injuries resulting from trauma, diseases or tumor surgery require grafts to bridge the proximal and distal

nerve ends. Autografts are the current gold standard, however is often limited in supply, requires a prolonged surgical time, and can cause donor site morbidity. As an alternative, several conduit materials both natural and synthetics have been used as a nerve graft. Several biodegradable polymers were successfully electrospun into nerve grafts and tested for their efficacy to stimulate axonal regeneration through its entire length (Ahmed *et al* 2006, Bellamkonda 2006, Bini *et al* 2006, Corey *et al* 2007 Epub ahead of print, Itoh *et al* 2006, Patel *et al* 2007, Schnell *et al* 2007, Yang *et al* 2004, 2005).

Several studies were carried out to see the effect of nanofiber diameter and alignment in terms of neurite outgrowth and neural stem cells (NSCs) differentiation. PLLA electrospun nanofibers of high, intermediate and random alignment showed varied responses to NSCs. Neurites grew radially outward from the ganglia on aligned fibers and turned to follow the fibers upon contact. Neurites on highly aligned substrates were longer than neurites on other fibers (Corey *et al* 2007 Epub ahead of print). NSC's elongation and its neurite outgrowth were in the direction of PLLA aligned nanofibers (Yang *et al* 2004), and the rate of NSC differentiation was higher on PLLA nanofibers than on PLLA microfibers (Yang *et al* 2005). Surface-modified PLLA electrospun aligned nanofiber matrices with ECM proteins and bFGF growth factor simulate the natural ECM environment by providing necessary physical and chemical cues (Patel *et al* 2007). The aligned nanofibers significantly induced the neurite outgrowth compared to randomly oriented nanofibers. Figure 7 represents the confocal images of neurites on nanofiber scaffolds oriented in the direction of aligned nanofibers and more branching on random nanofibers (Patel *et al* 2007). Reduced neurite branching on the aligned nanofiber matrices is highly encouraging in developing nerve graft substitutes.

PLAGA nanofibers and microfibers in the form of microbraided and aligned microfiber scaffolds supported the neurite outgrowth and NSCs differentiated in the direction of fiber alignment (Bini *et al* 2006). PCL and collagen/PCL (C/PCL 25:75 wt%) blend nanofibers both random and aligned nanofiber scaffolds supported cell attachment, Schwann cell migration and axonal regeneration (Schnell *et al* 2007). Glass coverslips coated with polyamide electrospun nanofibers in the diameter range of 100–800 nm supported neuronal attachment and neurite outgrowth *in vitro* (Ahmed *et al* 2006). Surface modification of these nanofibers with neuroactive peptides derived from human tenascin-C significantly enhanced the ability of the nanofibers to facilitate neuronal attachment, neurite generation and neurite extension *in vitro* compared to poly-L-lysine-coated coverslips (Ahmed *et al* 2006). Such an observed performance is presumably due to 3D nanofiber architecture and chemical cues that provide a more *in vivo* environment for neuronal growth. Blend nanofibers due to the presence of collagen showed significantly higher cellular activity, and neurites oriented in the direction of aligned nanofibers. In another study, electrospun chitosan nanofiber mesh tubes and tendon-chitosan tubes were employed for bridge grafting in the rat sciatic nerve model and autografts

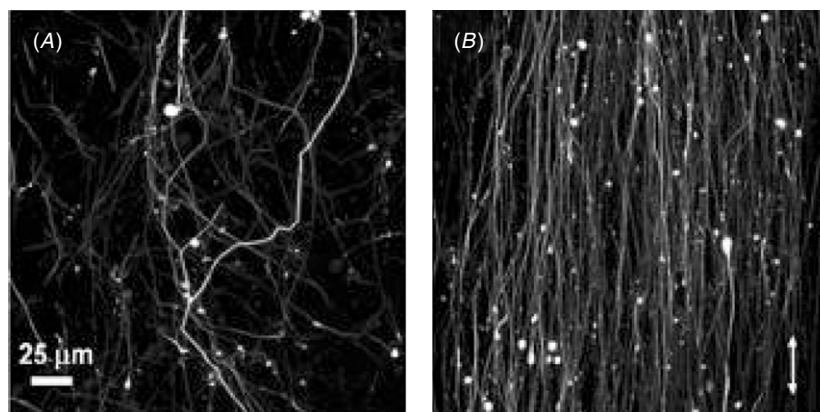


Figure 7. (A) and (B) High-magnification confocal microscopy images of neurite morphology on (A) random and (B) aligned surface modified PLLA nanofibers with bFGF. Neurites oriented in the direction of aligned nanofibers while more neurite branching on random nanofibers was seen. Reprinted with permission from Copyright © 2007 American Chemical Society (Patel *et al* 2007).

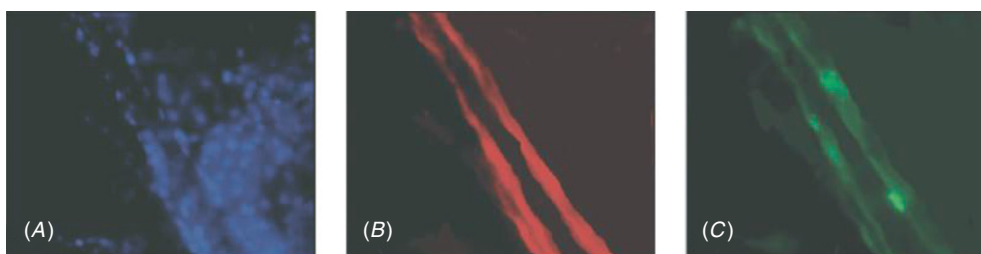


Figure 8. Myoblast differentiation on Matrigels-coated DegraPols slides in differentiation medium (2% HS). Upper lane: C2C12 cells. Hoechst-stained myoblast nuclei (A), F-actin stained with rhodamine-phalloidin (B), FITC-conjugated antibody for MHC (C). Lower: C2C12 myotubes aligned preferentially along the fiber length. Reprinted with permission from Copyright © 2005 Elsevier Ltd. (Riboldi *et al* 2005).

were used as control (Itoh *et al* 2006). Histological evaluations after four and eight weeks showed significantly improved performance for chitosan nanofiber mesh tube groups over both the tendon-chitosan tube and the autografts (Itoh *et al* 2006).

4.5. Electrospun nanofiber skeletal muscle grafts

Skeletal muscle comprises (Saxena *et al* 1999) approximately 48% of the body mass and control voluntary movement and maintenance of the structural contours (Cronin *et al* 2004, Riboldi *et al* 2005). Mature skeletal muscle tissue is composed of multinucleated, post-mitotic fibers that do not regenerate the following injury. Locally, quiescent populations of myogenic progenitors exist, that will fuse with existing or damaged myotubes to form new ones. In major injuries where the muscle structure is irreversibly compromised, engineered muscle constructs may overcome problems of muscle transfers and provide a successful replacement device for muscle regeneration.

Non-woven PGA fiber mesh (fiber diameter 12 μm) seeded with myoblasts isolated from rat pups were implanted in the omentum of adult fisher CDF-F344 male and female rats (Saxena *et al* 1999). This cell polymer constructs immunostained positively for alpha sacromeric actin and desmin; markers for skeletal muscle at both four and six weeks

post-implantation. Viable myoblasts were visualized along partially degraded PGA fibers by H&E staining.

Adhesion and proliferation of murine myoblast cell line (C2C12) on electrospun DegraPol (fiber diameter 10 μm) is comparable with tissue culture plastic, which is indicative of no toxicity and excellent cell compatibility (Riboldi *et al* 2005). In differentiation media, C2C12 cells seeded on Matrigel-coated DegraPol showed the presence of elongated, multinucleated, myosin-expressing myotubes. Immunofluorescence microscopy shows C2C12 myotubes aligned preferentially along the fiber length as visualized by staining of F-actin and myosin heavy chains as shown in figure 8.

C2C12 cells seeded onto a gelatin- or fibronectin-coated non-woven electrospun PLLA fiber mesh (fiber diameter 500 nm) showed disordered actin filament arrangement on randomly oriented fiber mesh, whereas actin fibers were aligned along the fiber direction on aligned fiber meshes (Huang *et al* 2006). Myotubes attached and formed multinucleated myofibers along the nanofiber direction globally after seven days in differentiation media. The highly organized myotubes on the aligned mesh were significantly longer than those on randomly oriented scaffolds and thus mimicked the longer and parallel myotubes assembly seen in native muscular tissue.

5. Conclusions

Electrospun nanofiber matrices show morphological similarities to the natural ECM comprising of ultrafine continuous fibers, high surface area, high porosity and variable pore-size distribution similar to the dimensions of basement membranes. These remarkable surface properties, combined with specific surface chemistry, provide cells a three-dimensional *in vivo* environment. Studies have clearly shown that nanofiber scaffolds significantly alter the cell behavior and perform better as scaffold materials to regenerate various tissues.

Efforts are being made to improve mechanical properties of electrospun nanofibers to match the native tissue by a combination of several polymers, fiber diameter and fiber orientation. In some studies combining natural polymers and proteins with synthetic polymers altered the surface properties resulting in improved cell behavior. Fiber diameter and orientation also had a significant effect on cellular response. Such changes in observed cellular behavior might be due to the changes in surface properties such as hydrophilicity, roughness and changes in porosity and pore diameter. Such changes in surface properties can lead to adsorption of more ECM proteins such as vitronectin, fibronectin etc and result in improved cell adhesion and proliferation compared to flat or 2D surfaces. In addition, higher porosity and wide pore diameters resulting from combination of micro-nanofibers showed encouraging cell infiltration into the 3D construct. All of these properties need to be considered while constructing nanofiber-based grafts for tissue regeneration.

In general, electrospinning utilizes several fluorinated and toxic organic solvents to dissolve polymers. Such toxic solvents might affect the structural conformation of several biopolymers and proteins and result in undesired cellular response. A critical need exists to replace these toxic organic solvents with aqueous based or less toxic solvents during electrospinning. Also more efforts need to be made to improve efficiency of nanofiber production, packing, shipping and handling. Such efforts can further improve the efficacy of nanofibers, and can lead to the development of commercially viable nanofiber technology for a variety of biomedical applications.

Acknowledgment

The authors gratefully acknowledge funding from the NIH (R01 EB004051 and R01 AR052536). Dr Laurencin was the recipient of a Presidential Faculty Fellow Award from the National Science Foundation.

References

- Abrams G A, Goodman S L, Nealey P F, Franco M and Murphy C J 2000 Nanoscale topography of the basement membrane underlying the corneal epithelium of the rhesus macaque *Cell Tissue Res.* **299** 39–46
- Abrams G A, Murphy C J, Wang Z Y, Nealey P F and Bjorling D E 2003 Ultrastructural basement membrane topography of the bladder epithelium *Urol. Res.* **31** 341–6
- Adams J C 2001 Cell–matrix contact structures *Cell. Mol. Life Sci.* **58** 371–92
- Ahmed I, Liu H, Mamiya P C, Ponery A S, Babu A N, Weik T, Schindler M and Meiners S 2006 Three-dimensional nanofibrillar surfaces covalently modified with tenascin-C-derived peptides enhance neuronal growth *in vitro* *J. Biomed. Mater. Res. A* **76** 851–60
- Ahmed I, Ponery A S, Nur-E-Kamal A, Kamal J, Meshel A S, Sheetz M P, Schindler M and Meiners S 2007 Morphology, cytoskeletal organization, and myosin dynamics of mouse embryonic fibroblasts cultured on nanofibrillar surfaces *Mol. Cell. Biochem.* **301** 241–9
- Bellamkonda R V 2006/7 Peripheral nerve regeneration: An opinion on channels, scaffolds and anisotropy *Biomaterials* **27** 3515–8
- Berne R W 2004 Towards the conscientious development of ethical nanotechnology *Sci. Eng. Ethics* **10** 627–38
- Bhattacharyya S, Kumbar S G, Khan Y M, Nair L S and Laurencin C T 2006 Fabrication and biocompatibility of polyphosphazene tubular electrospun nanofiber scaffolds for bone tissue engineering *Proc. 2006 Summer Bioengineering Conf. on Podium: 12A Tissue Eng./Biomechanics II: Orthopaedic Apps (Amelia Island, Florida, 21–25 June 2006)*
- Bhattarai S R, Bhattarai N, Yi H K, Hwang P H, Cha D I and Kim H Y 2004 Novel biodegradable electrospun membrane: scaffold for tissue engineering *Biomaterials* **25** 2595–602
- Bini T B, Gao S, Wang S and Ramakrishna S 2006 Poly(l-lactide-co-glycolide) biodegradable microfibers and electrospun nanofibers for nerve tissue engineering: an *in vitro* study *J. Mater. Sci.* **41** 6453–9
- Burger C, Hsiao B S and Chu B 2006 Nanofibrous materials and their applications *Annu. Rev. Mater. Res.* **36** 333–68
- Buttafoco L, Kolkman N G, Engbers-Buijtenhuijs P, Poot A A, Dijkstra P J, Vermes I and Feijen J 2006 Electrospinning of collagen and elastin for tissue engineering applications *Biomaterials* **27** 724–34
- Cao Y, Liu Y, Liu W, Shan Q, Buonocore S D and Cui L 2002 Bridging tendon defects using autologous tenocyte engineered tendon in a hen model *Plast. Reconstr. Surg.* **110** 1280–9
- Cao D, Liu W, Wei X, Xu F, Cui L and Cao Y 2006 *In vitro* tendon engineering with avian tenocytes and polyglycolic acids: a preliminary report *Tissue Eng.* **12** 1369–77
- Chen C S, Mrksich M, Huang S, Whitesides G M and Ingber D E 1997 Geometric control of cell life and death *Science* **276** 1425–8
- Chew S Y, Wen Y, Dzenis Y and Leong K W 2006 The role of electrospinning in the emerging field of nanomedicine *Curr. Pharm. Des.* **12** 4751–70
- Chiquet M 1999 Regulation of extracellular matrix gene expression by mechanical stress *Matrix Biol.* **18** 417–26
- Chiu J B, Luu Y K, Fang D, Hsiao B S, Chu B and Hadjiargyrou M 2005 Electrospun nanofibrous scaffolds for biomedical applications *J. Biomed. Nanotechnol.* **1** 115–32
- Chong E J, Phan T T, Lim I J, Zhang Y Z, Bay B H, Ramakrishna S and Lim C T 2007 Evaluation of electrospun PCL/gelatin nanofibrous scaffold for wound healing and layered dermal reconstitution *Acta Biomater.* **3** 321–30
- Chou L, Firth J D, Uitto V J and Brunette D M 1998 Effects of titanium substratum and grooved surface topography on metalloproteinase-2 expression in human fibroblasts *J. Biomed. Mater. Res.* **39** 437–45
- Corey J M, Lin D Y, Mycek K B, Chen Q, Samuel S, Feldman E L and Martin D C 2007 Aligned electrospun nanofibers specify the direction of dorsal root ganglia neurite growth *J. Biomed. Mater. Res. A* **83** 636–45
- Cronin E M, Thurmond F A, Bassel-Duby R, Williams R S, Wright W E, Nelson K D and Garner H R 2004 Protein-coated poly(L-lactic acid) fibers provide a substrate for differentiation of human skeletal muscle cells *J. Biomed. Mater. Res. A* **69** 373–81
- Dalby M J, Yarwood S J, Riehle M O, Johnstone H J, Affrossman S and Curtis A S 2002 Increasing fibroblast response to materials

- using nanotopography: morphological and genetic measurements of cell response to 13-nm-high polymer demixed islands *Exp. Cell Res.* **276** 1–9
- Dalton P D, Klee D and Möller M 2005 Electrospinning with dual collection rings *Polymer* **46** 611–4
- Deitzel J M, Kleinmeyer J, Harris D and Beck Tan N C 2001 The effect of processing variables on the morphology of electrospun nanofibers and textiles *Polymer* **42** 261–72
- Duan B, Wu L, Yuan X, Hu Z, Li X, Zhang Y, Yao K and Wang M 2007 Hybrid nanofibrous membranes of PLGA/chitosan fabricated via an electrospinning array *J. Biomed. Mater. Res. A* **83** 868–78
- Fang Y, Xu Y and He P 2005 DNA biosensors based on metal nanoparticles *J. Biomed. Nanotechnol.* **1** 276–85
- Fridrikh S V, Yu J H, Brenner M P and Rutledge G C 2003 Controlling the fiber diameter during electrospinning *Phys. Rev. Lett.* **90** 144502
- Funakoshi T, Majima T, Suenaga N, Iwasaki N, Yamane S and Minami A 2006 Rotator cuff regeneration using chitin fabric as an acellular matrix *J. Shoulder Elbow Surg.* **15** 112–8
- Glass-Brudzinski J, Perizzolo D and Brunette D M 2002 Effects of substratum surface topography on the organization of cells and collagen fibers in collagen gel cultures *J. Biomed. Mater. Res.* **61** 608–18
- He W, Yong T, Ma Z W, Inai R, Teo W E and Ramakrishna S 2006 Biodegradable polymer nanofiber mesh to maintain functions of endothelial cells *Tissue Eng.* **12** 2457–66
- He W, Yong T, Teo W E, Ma Z and Ramakrishna S 2005 Fabrication and endothelialization of collagen-blended biodegradable polymer nanofibers: potential vascular graft for blood vessel tissue engineering *Tissue Eng.* **11** 1574–88
- Hohman M M, Shin M, Rutledge G and Brenner M P 2001a Electrospinning and electrically forced jets: I. Stability theory *Phys. Fluids* **13** 2201–20
- Hohman M M, Shin M, Rutledge G and Brenner M P 2001b Electrospinning and electrically forced jets: II. Applications *Phys. Fluids* **13** 2221–36
- Huang N F, Patel S, Thakar R G, Wu J, Hsiao B S, Chu B, Lee R J and Li S 2006 Myotube assembly on nanofibrous and micropatterned polymers *Nano Lett.* **6** 537–42
- Huang Z, Zhang Y, Kotaki M and Ramakrishna S 2003 A review on polymer nanofibers by electrospinning and their applications in nanocomposites *Comp. Sci. Technol.* **63** 2223–53
- Ishii O, Shin M, Sueda T and Vacanti J P 2005 *In vitro* tissue engineering of a cardiac graft using a degradable scaffold with an extracellular matrix-like topography *J. Thorac. Cardiovasc. Surg.* **130** 1358–63
- Itoh S, Wang W, Matsuda A, Shinomiya K, Hata Y and Tanaka J 2006 Efficacy of chitosan nanofiber mesh as a scaffold for regenerating nerve tissue *Kichin, Kitosan Kenkyu* **12** 194–5
- Jayasinghe S N, Irvine S and McEwan J R 2007 Cell electrospinning highly concentrated cellular suspensions containing primary living organisms into cell-bearing threads and scaffolds *Nanomedicine* **2** 555–67
- Jayasinghe S N, Qureshi A N and Eagles P A 2006 Electrohydrodynamic jet processing: an advanced electric-field-driven jetting phenomenon for processing living cells *Small* **2** 216–9
- Jeong S I, Kim S Y, Cho S K, Chong M S, Kim K S, Kim H, Lee S B and Lee Y M 2007 Tissue-engineered vascular grafts composed of marine collagen and PLGA fibers using pulsatile perfusion bioreactors *Biomaterials* **28** 1115–22
- Jiang H, Hu Y, Li Y, Zhao P, Zhu K and Chen W 2005 A facile technique to prepare biodegradable coaxial electrospun nanofibers for controlled release of bioactive agents *J. Control. Release* **108** 237–43
- Karuri N W, Liliensiek S, Teixeira A I, Abrams G, Campbell S, Nealey P F and Murphy C J 2004 Biological length scale topography enhances cell-substratum adhesion of human corneal epithelial cells *J. Cell. Sci.* **117** 3153–64
- Katti D S, Robinson K W, Ko F K and Laurencin C T 2004 Bioresorbable nanofiber-based systems for wound healing and drug delivery: optimization of fabrication parameters *J. Biomed. Mater. Res. B. Appl. Biomater.* **70** 286–96
- Khil M S, Cha D I, Kim H Y, Kim I S and Bhattarai N 2003 Electrospun nanofibrous polyurethane membrane as wound dressing *J. Biomed. Mater. Res. B. Appl. Biomater.* **67** 675–9
- Kim S J, Lee C K and Kim S I 2005 Effect of ionic salts on the processing of poly(2-acrylamido-2-methyl-1-propane sulfonic acid) nanofibers *J. Appl. Polym. Sci.* **96** 1388–93
- Kim S H, Nam Y S, Lee T S and Park W H 2003 Silk fibroin nanofiber Electrospinning, properties, and structure *Polym. J.* **35** 185–90
- Kumbar S G, Bhattacharyya S, Sethuraman S and Laurencin C T 2007a A preliminary report on a novel electrospray technique for nanoparticle based biomedical implants coating: precision electrospinning *J. Biomed. Mater. Res. B. Appl. Biomater.* **81** 91–103
- Kumbar S G, James R, Nair L S and Laurencin C T 2007b Nanotechnology for inducing angiogenesis *Micro- and Nanoengineering of the Cell Microenvironment: Technologies and Applications* ed A Khademhosseini, J Borenstein, S Takayama and M Toner (Norwood, MA: Artech House)
- Kumbar S G, Kofron M D, Nair L S and Laurencin C T 2008 Cell behavior toward nanostructured surfaces *Biomedical Nanostructures* ed K E Gonsalves, C T Laurencin, C Halberstadt and L S Nair (New York: Wiley) pp 257–91
- Kumbar S G, Nair L S, Bhattacharyya S and Laurencin C T 2006 Polymeric nanofibers as novel carriers for the delivery of therapeutic molecules *J. Nanosci. Nanotechnol.* **6** 2591–607
- Kumbar S G, Nukavarapu S P, James R, Nair L S and Laurencin C T 2007c Nanobased fiber matrices for wound repair: optimization for human skin fibroblast growth *Podium* No 34
- Kwon O H, Lee I S, Ko Y, Meng W, Jung K, Kang I and Ito Y 2007 Electrospinning of microbial polyester for cell culture *Biomed. Mater.* **2** S52–8
- Laurencin C T and Nair L S 2004 Polyphosphazene nanofibers for biomedical applications: preliminary studies *NATO Science Series: II. Mathematics, Physics and Chemistry (Nanoengineered Nanofibrous Materials vol 169)* (Norwell, MA: Kluwer Academic) pp 283–302
- Li D, Ouyang G, McCann J T and Xia Y 2005 Collecting electrospun nanofibers with patterned electrodes *Nano Lett.* **5** 913–6
- Li D, Wang Y and Xia Y 2004 Electrospinning nanofibers as uniaxially aligned arrays and layer-by-layer stacked films *Adv. Mater.* **16** 361–6
- Li W J, Laurencin C T, Caterson E J, Tuan R S and Ko F K 2002 Electrospun nanofibrous structure: a novel scaffold for tissue engineering *J. Biomed. Mater. Res.* **60** 613–21
- Li W J, Mauck R L, Cooper J A, Yuan X and Tuan R S 2007 Engineering controllable anisotropy in electrospun biodegradable nanofibrous scaffolds for musculoskeletal tissue engineering *J. Biomech.* **40** 1686–93
- Liao S, Li B, Ma Z, Wei H, Chan C and Ramakrishna S 2006 Biomimetic electrospun nanofibers for tissue regeneration *Biomed. Mater.* **1** R45–53
- Liu X, Smith L, Wei G, Won Y and Ma P X 2005 Surface engineering of nano-fibrous poly (L-lactic acid) scaffolds via self-assembly technique for bone tissue engineering *J. Biomed. Nanotechnol.* **1** 54–60
- Ma Z, Kotaki M, Yong T, He W and Ramakrishna S 2005 Surface engineering of electrospun polyethylene terephthalate (PET) nanofibers towards development of a new material for blood vessel engineering *Biomaterials* **26** 2527–36
- MacNeil S 2007 Progress and opportunities for tissue-engineered skin *Nature* **445** 874–80

- Min B M, Jeong L, Lee K Y and Park W H 2006 Regenerated silk fibroin nanofibers: water vapor-induced structural changes and their effects on the behavior of normal human cells *Macromol. Biosci.* **6** 285–92
- Min B M, Lee G, Kim S H, Nam Y S, Lee T S and Park W H 2004 Electrospinning of silk fibroin nanofibers and its effect on the adhesion and spreading of normal human keratinocytes and fibroblasts *in vitro* *Biomaterials* **25** 1289–97
- Nain A S, Wong J C, Amon C and Sitti M 2006 Drawing suspended polymer micro/nanofibers using glass micropipettes *Appl. Phys. Lett.* **89** 183105–7
- Nalwa H S 2000 *Handbook of Nanostructured Materials and Nanotechnology* (San Diego, CA: Academic Press)
- Noh H K, Lee S W, Kim J, Oh J, Kim K, Chung C, Choi S, Park W H and Min B 2006 Electrospinning of chitin nanofibers: degradation behavior and cellular response to normal human keratinocytes and fibroblasts *Biomaterials* **27** 3934–44
- Nukavarapu S P, Kumbar S G, Nair L S and Laurencin C T 2008 *Nanostructures for Tissue Engineering/Regenerative Medicine* ed K E Gonsalves, C T Laurencin, C Halberstadt and L S Nair (New York: Wiley) pp 371–401
- Ouyang H W, Goh J C, Mo X M, Teoh S H and Lee E H 2002 The efficacy of bone marrow stromal cell-seeded knitted PLGA fiber scaffold for achilles tendon repair *Ann. NY Acad. Sci.* **961** 126–9
- Ouyang H W, Goh J C, Thambyah A, Teoh S H and Lee E H 2003 Knitted poly-lactide-co-glycolide scaffold loaded with bone marrow stromal cells in repair and regeneration of rabbit Achilles tendon *Tissue Eng.* **9** 431–9
- Pan H, Jiang H and Chen W 2006 Interaction of dermal fibroblasts with electrospun composite polymer scaffolds prepared from dextran and poly lactide-co-glycolide *Biomaterials* **27** 3209–20
- Paramonov S E, Jun H W and Hartgerink J D 2006 Self-assembly of peptide-amphiphile nanofibers: the roles of hydrogen bonding and amphiphilic packing *J. Am. Chem. Soc.* **128** 7291–8
- Park K E, Jung S Y, Lee S J, Min B and Park W H 2006 Biomimetic nanofibrous scaffolds: Preparation and characterization of chitin/silk fibroin blend nanofibers *Int. J. Biol. Macromol.* **38** 165–73
- Patel S, Kurpinski K, Quigley R, Gao H, Hsiao B S, Poo M and Li S 2007 Bioactive nanofibers: synergistic effects of nanotopography and chemical signaling on cell guidance *Nano Lett.* **7** 2122–8
- Peppas N A, Hilt J Z and Thomas J B (ed) 2007 *Nanospheres of Intelligent Networks for Biomedical and Drug Delivery Applications. Nanotechnology in Therapeutics* (Wymondham, UK: Horizon Bioscience) pp 361–79
- Recker D H, Yarin A L, Fong H and Koombhongse S 2000 Bending instability of electrically charged liquid jets of polymer solutions in electrospinning *J. Appl. Phys.* **87** 4531–47
- Rho K S, Jeong L, Lee G, Seo B M, Park Y J, Hong S D, Roh S, Cho J J, Park W H and Min B M 2006 Electrospinning of collagen nanofibers: effects on the behavior of normal human keratinocytes and early-stage wound healing *Biomaterials* **27** 1452–61
- Riboldi S A, Sampaolesi M, Neuenschwander P, Cossu G and Mantero S 2005 Electrospun degradable polyesterurethane membranes: potential scaffolds for skeletal muscle tissue engineering *Biomaterials* **26** 4606–15
- Sahoo S, Ouyang H, Goh J C, Tay T E and Toh S L 2006 Characterization of a novel polymeric scaffold for potential application in tendon/ligament tissue engineering *Tissue Eng.* **12** 91–9
- Sato M, Maeda M, Kurosawa H, Inoue Y, Yamauchi Y and Iwase H 2000 Reconstruction of rabbit Achilles tendon with three bioabsorbable materials: histological and biomechanical studies *J. Orthop. Sci.* **5** 256–67
- Saxena A K, Marler J, Benvenuto M, Willital G H and Vacanti J P 1999 Skeletal muscle tissue engineering using isolated myoblasts on synthetic biodegradable polymers: preliminary studies *Tissue Eng.* **5** 525–32
- Schnell E, Klinkhammer K, Balzer S, Brook G, Klee D, Dalton P and Mey J 2007 Guidance of glial cell migration and axonal growth on electrospun nanofibers of poly- ϵ -caprolactone and a collagen/poly- ϵ -caprolactone blend *Biomaterials* **28** 3012–25
- Shin Y M, Hohman M M, Brenner M P and Rutledge G C 2001 Experimental characterization of electrospinning: the electrically forced jet and instabilities *Polymer* **42** 9955–67
- Shin M, Ishii O, Sueda T and Vacanti J P 2004 Contractile cardiac grafts using a novel nanofibrous mesh *Biomaterials* **25** 3717–23
- Stankus J J, Guan J, Fujimoto K and Wagner W R 2006 Microintegrating smooth muscle cells into a biodegradable, elastomeric fiber matrix *Biomaterials* **27** 735–44
- Stitzel J *et al* 2006 Controlled fabrication of a biological vascular substitute *Biomaterials* **27** 1088–94
- Streuli C 1999 Extracellular matrix remodelling and cellular differentiation *Curr. Opin. Cell Biol.* **11** 634–40
- Sun T, Mai S, Norton D, Haycock J W, Ryan A J and MacNeil S 2005 Self-organization of skin cells in three-dimensional electrospun polystyrene scaffolds *Tissue Eng.* **11** 1023–33
- Tao S L and Desai T A 2007 Aligned arrays of biodegradable poly(ϵ -caprolactone) nanowires and nanofibers by template synthesis *Nano Lett.* **7** 1463–8
- Theron A, Zussman E and Yarin A L 2001 Electrostatic field-assisted alignment of electrospun nanofibres *Nanotechnology* **12** 384–90
- Venugopal J, Ma L L, Yong T and Ramakrishna S 2005 *In vitro* study of smooth muscle cells on polycaprolactone and collagen nanofibrous matrices *Cell Biol. Int.* **29** 861–7
- Venugopal J and Ramakrishna S 2005 Biocompatible nanofiber matrices for the engineering of a dermal substitute for skin regeneration *Tissue Eng.* **11** 847–54
- Vitte J, Benoliel A M, Pierres A and Bongrand P 2004 Is there a predictable relationship between surface physical-chemical properties and cell behaviour at the interface? *Eur. Cell. Mater.* **7** 52, 63, discussion 63
- Ward G F 2001 Meltblown nanofibres for nonwoven filtration applications *Filtration Separation* **38** 42–3
- Watanabe M *et al* 2001 Tissue-engineered vascular autograft: inferior vena cava replacement in a dog model *Tissue Eng.* **7** 429–39
- Watt F M 1986 The extracellular matrix and cell shape *Trends Biochem. Sci.* **11** 482–5
- Xu C Y, Inai R, Kotaki M and Ramakrishna S 2004 Aligned biodegradable nanofibrous structure: a potential scaffold for blood vessel engineering *Biomaterials* **25** 877–86
- Yang F, Xu C Y, Kotaki M, Wang S and Ramakrishna S 2004 Characterization of neural stem cells on electrospun poly(L-lactic acid) nanofibrous scaffold *J. Biomater. Sci., Poly. Ed.* **15** 1483–97
- Yang F, Murugan R, Wang S and Ramakrishna S 2005 Electrospinning of nano/micro scale poly(L-lactic acid) aligned fibers and their potential in neural tissue engineering *Biomaterials* **26** 2603–10
- Yarin A L, Koombhongse S and Recker D H 2001a Taylor cone and jetting from liquid droplets in electrospinning of nanofibers *J. Appl. Phys.* **90** 4836–46
- Yarin A L, Koombhongse S and Recker D H 2001b Bending instability in electrospinning of nanofibers *J. Appl. Phys.* **89** 3018–26
- Zhang Q, Chang Z, Zhu M, Mo X and Chen D 2007 Electrospun carbon nanotube composite nanofibres with uniaxially aligned arrays *Nanotechnology* **18** 115611–6

- Zhang Y, Lim C T, Ramakrishna S and Huang Z M 2005a Recent development of polymer nanofibers for biomedical and biotechnological applications *J. Mater. Sci. Mater. Med.* **16** 933–46
- Zhang Y Z, Venugopal J, Huang Z M, Lim C T and Ramakrishna S 2005b Characterization of the surface biocompatibility of the electrospun PCL-collagen nanofibers using fibroblasts *Biomacromolecules* **6** 2583–9
- Zhong S, Teo W E, Zhu X, Beuerman R W, Ramakrishna S and Yung L Y 2006 An aligned nanofibrous collagen scaffold by electrospinning and its effects on *in vitro* fibroblast culture *J. Biomed. Mater. Res. A* **79** 456–63
- Zong X, Bien H, Chung C Y, Yin L, Fang D, Hsiao B S, Chu B and Entcheva E 2005 Electrospun fine-textured scaffolds for heart tissue constructs *Biomaterials* **26** 5330–8
- Zong X, Li S, Chen E, Garlick B, Kim K-S, Fang D, Chiu J, Zimmerman T, Brathwaite C, Hsiao B S and Chu B 2004 Prevention of postsurgery-induced abdominal adhesions by electrospun bioabsorbable nanofibrous poly (lactide-co-glycolide)- based membranes *Ann. Surg.* **240** 910–5